International Journal of Applied Earth Observation and Geoinformation 11 (2009) 27–37

Contents lists available at ScienceDirect

International Journal of Applied Earth Observation and Geoinformation

journal homepage: www.elsevier.com/locate/jag

Linking socioeconomic classes and land cover data in Lima, Peru: Assessment through the application of remote sensing and GIS

Silvania Avelar [a,*], Rainer Zah [a,1], Carlos Tavares-Corrêa [b,2]

[a] Technology and Society Laboratory, Swiss Federal Laboratories for Materials Testing and Research (Empa), Überlandstrasse 129, CH-8600 Dübendorf, Switzerland
[b] Applied Geography Research Center, Pontifical Catholic University of Peru (PUCP), Av. Universitaria 1801, San Miguel, Lima 32, Peru

ARTICLE INFO

Article history:
Received 2 April 2007
Accepted 12 May 2008

Keywords:
Socioeconomic classes
Supervised classification
GIS analysis
Grid-based approach
Accuracy assessment

ABSTRACT

The spatial differentiation of socioeconomic classes in a city can deliver insight into the nexus of urban development and the environment. The purpose of this paper is to identify poor and rich regions in large cities according to the predominant physical characteristics of the regions. Meaningful spatial information from urban systems can be derived using remote sensing and GIS tools, especially in large difficult-to-manage cities where the dynamics of development results in rapid changes to urban patterns. We use here very high resolution imagery data for the identification of homogeneous socioeconomic zones in a city. We formulate the categorization task as a GIS analysis of an image classified with conventional techniques. Experiments are conducted using a QuickBird image of a study area in Lima, Peru. We provide accuracy assessment of results compared to ground truth data. Results show an approximated allocation of socioeconomic zones within Lima. The methodology described could also be applied to other urban centers, particularly large cities of Latin America, which have characteristics similar to those of the study area.

1. Introduction

Today almost half of the world's population lives in urban areas, and the prospect is that 60% of the world's population will be urban by 2030 (UN, 2006). Most of this urban growth will take place in developing countries and the number of megacities will increase to 100 by 2025 (Wang and Quattrochi, 2007). One of the many problems resulting from this rapid urban growth is the environmental impact it will have on air, water and soils, especially in the less developed areas of the planet. More and more evidence is emerging that air and water pollution, wastes, water infiltration, energy consumption, climate change, and biodiversity in cities have influences on the environment that go beyond the urban dimension and affect the regional, national and global levels. However, governmental methods of monitoring and available environmental data are currently insufficient to support measures and preventive actions. New and faster methods of monitoring are required to generate adequate data to help link the location and degree of environmental impacts in urban systems to local policies and controlling actions.

The distribution of socioeconomic classes within large cities is an important factor in understanding the urban environmental conditions in large cities. Finding such spatial patterns makes it possible to correlate them with the available infrastructure facilities and environmental loads in different parts of the city. This can help us understand the vulnerability aspects of the urban environment and the population. For example, socioeconomic classes and their census characteristics can be related to spatially derived indicators such as data on public services and transportation (energy consumption, water, public transport, traffic congestion), health and sanitation (air pollution, waste disposal, infectious diseases, medical services), the natural environment (record of natural disasters, climate), and security (crimes, policing). The development of such environmental profiles of cities can help to assess and prioritize local environmental issues in urban monitoring.

Urban studies in the last two decades have focused mainly on social science issues such as poverty, social exclusion and employment promotion. There is a lack of research on stratification and socioeconomic classes in large cities, especially in Latin America (Sembler, 2006). This paper is intended to help reduce that lack of information by investigating the spatial distribution of socioeconomic classes in a large city in South America.

Remote sensing can be used to provide up-to-date spatial information of a wide variety of urban phenomena at multiple resolutions (Jensen and Cowen, 1999; Herold et al., 2007).

* Corresponding author. Tel.: +41 44 823 4423; fax: +41 71 2747862.
E-mail address: silvania.avelar@empa.ch (S. Avelar).
[1] Tel.: +41 823 4604; fax: +41 44 8234042.
[2] Tel.: +51 1 626 2000x4530, 4530; fax: +51 1 6262804.

0303-2434/$ – see front matter © 2008 Elsevier B.V. All rights reserved.
doi:10.1016/j.jag.2008.05.001

However, the accurate classification of urban land cover and land use categories from very high resolution (better than 1 m) imagery data remains a challenge (Sutton et al., 2007; Fox et al., 2003). The reason is that it is difficult to define suitable training sets in very high resolution satellite imagery data for a supervised classification, because various land cover types co-exist and alternate frequently. For example, streets, sidewalks, houses, trees, bare soil, and swimming pools, and their elements themselves present heterogeneity, such as a road with cars, resulting in distinct spectral variation within areas of homogeneous land cover classes (Taubenbock et al., 2006). Additional difficulties arise when considering the dissimilarity of functions for inferring urban land use, such as residential or industrial areas, parks or agricultural fields. Since land use describes the same land cover features in terms of their function or socioeconomic significance, it may be possible to infer land use from land cover observations. For example, land use classes of gardens, houses, and canals may refer to land cover classes of vegetation, buildings, and water, respectively. Therefore, the distinction between land cover and land use has often been overlooked in urban studies (Mesev, 2003). Several techniques have been employed or developed to classify urban images, considering various class boundaries and within-class variances. These techniques include object based classification algorithms (e.g. Taubenbock et al., 2006), neural networks (e.g. Zhang and Foody, 2001), non-linear regression (e.g. Landis et al., 2005), and statistical algorithms (e.g. Stefanov et al., 2001).

In this paper we want to answer the question as to whether it is possible to estimate different socioeconomic classes for an urban area from very high resolution satellite image data using traditional statistical algorithms for supervised classification and GIS tools. A major goal of the study was also to determine and track relationships between land cover data and socioeconomic classes. Using GIS, we seek to construct a modelling method that can be replicated and applied to other urban centers with similar characteristics as the study area. Although urban areas vary considerably according to land use and location and an urban classification analysis should always consider the context of the study area.

2. Study area and data used

2.1. Description of study area

The study was carried out in a 9 km × 10 km area located in the south of Lima, Peru. Lima is the 30th most populated city of the world with a population of over 7 million inhabitants (UN, 2006). As has been the case with most large cities in Latin America, high rates of population growth and rural–urban migration have been the most important factors in the growth and expansion of the city of Lima. The spatial pattern of growth is marked by a peripherization process. This means that the growth process is characterized by an expansion of the borders of the city through the massive formation of peripheral settlements, which are in most cases low-income residential areas (Barros, 2004). The study area includes the neighboring districts of Santiago de Surco and San Juan de Miraflores. This area was chosen because it has widely divergent human activities and social classes. Furthermore, these districts border on peripheral settlements which have expanded over adjacent agricultural land and non-urban hills. Fig. 1 illustrates the contrasting social classes found in the study area.

As Lima is situated in one of the driest regions of the planet (Lyndolph, 1973), vegetation can only be maintained with the aid of irrigation. Therefore, green areas exist only in high income parts of the city. Slums in Lima are not at all associated with green areas and as usual have very bad urban infrastructure, because they are informal settlements (Shutz, 1996). Houses in the slums are often unfinished and made with low-quality materials such as tin, straw, weathered wood and asbestos cloth (see Fig. 1). They are frequently connected to similar constructions around them, such that the housing density is high and the size of housing units in the

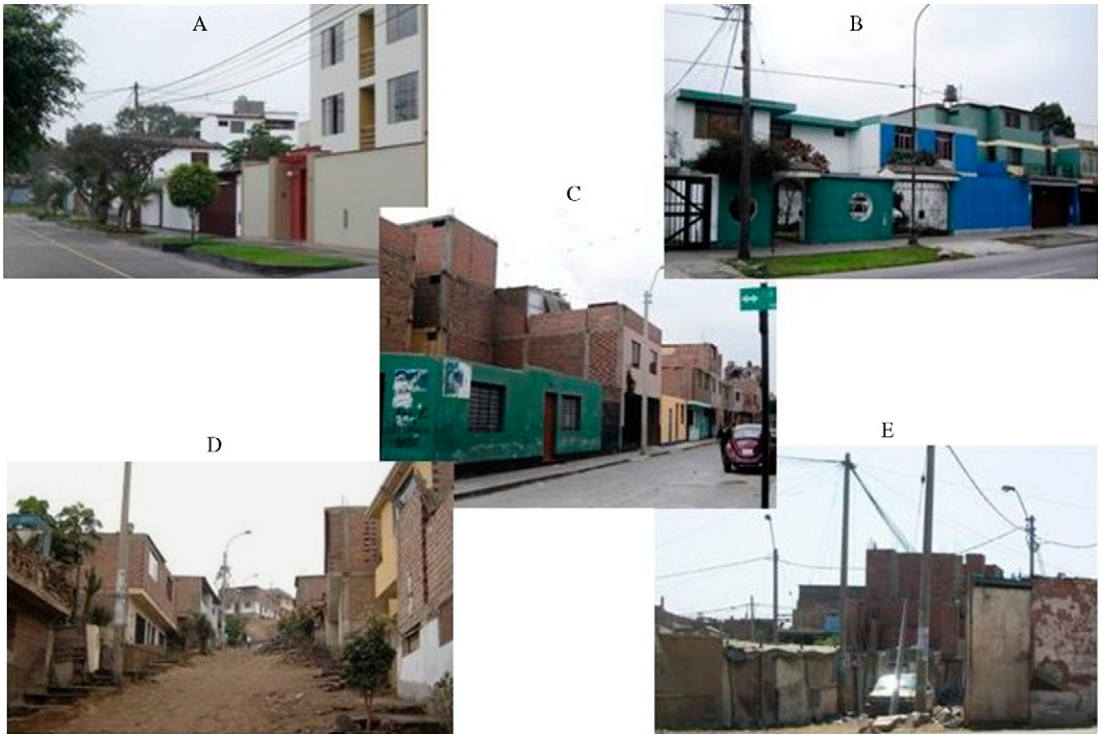

Fig. 1. Examples of habitations in Lima: high income area (A), middle income areas (B and C) and slums (D and E).

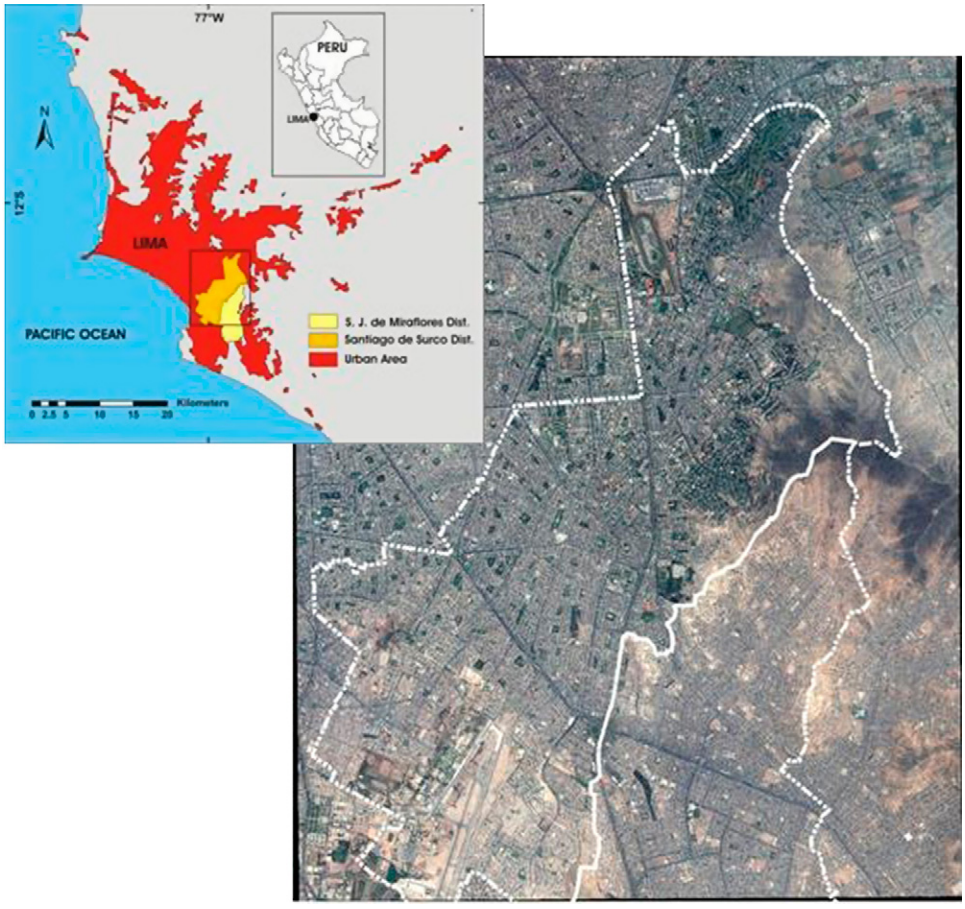

Fig. 2. Location of the study area in Lima, Peru, and preview of it in the QuickBird image (copyright by Eurimage).

area is fairly small. The roofs of houses in slums are usually made with the same material of the walls, but it is common to find houses without roof or ceiling in the newest invaded areas. Houses of the middle class can also be under construction, but they are typically 2-storey houses with walls of brick and unfinished concrete roofs on the top floor.

The location of the study area in Lima is shown in Fig. 2. The mountain in the center eastern sector of the study area is a site with high income houses on one side and slums on the other side. Middle class constructions are located mainly in the central left part of the study area. Industries can be found clustered in the inferior sector of the study area.

2.2. Data sets

2.2.1. Satellite data

A suitable satellite image for urban studies should show features in enough detail for the required analysis. Therefore, a QuickBird satellite image of the study area was chosen. The image was acquired on February 28, 2005. The spatial resolution of QuickBird imagery data is 0.6 m for panchromatic and 2.4 m for multispectral images. The high spatial resolution makes it possible to distinguish among constructions small in size, thus providing a survey of small built-up elements. QuickBird multispectral images have three visible bands (blue: 0.45–0.52 μm, green: 0.52–0.60 μm, red: 0.63–0.69 μm) and one near infrared band (0.76–0.90 μm). The radiometric resolution of QuickBird data is 11-bit digitization, which produces discernible intensity levels (up to 2048 levels).

2.2.2. Ground truth

Ground data for the study area was collected by a ground truth team in Lima to categorize regions according to their physical characteristics and socioeconomic classes. A ve-class scale ranging from A to E was applied: the A social class standing for richest and the E social class for poorest. The socioeconomic classes were identified based on observations of building characteristics (size, number of floors and building density), presence or absence of green areas, street pavement and land use. These characteristics are additional to the usual statistical census information gathered on social classes, which in Lima has the following average data (APOYO, 2005a,b):

- Class A: 3.6 members per family; monthly income over USD 2712.00; food and transportation expenses over USD 573.00; large 2-floor houses with, at least, 3 bedrooms and 4 bathrooms; private green areas in the backyard, front or both, garage for 2 or more cars and swimming pool; big walls and fences for protection; streets paved with asphalt.
- Class B: 4.1 members per family; monthly income from USD 745.00 to USD 2712.00; food and transportation expenses between USD 573.00 and 230.00; medium size 2-storey houses with 2.7 bedrooms and 2 bathrooms; some private green area, garage for 1 or 2 cars and often a small swimming pool; walls and fences for protection; streets paved with asphalt.
- Class C: 4.5 members per family; monthly income between USD 745.00 and USD 325.00; food and transportation expenses between USD 230.00 and 190.00; small to medium size 2-storey

houses with 2.3 bedrooms and 1.2 bathrooms; infrequently a garden, garage or swimming pool; terrain almost completely built; streets paved with low quality asphalt.
- Class D: 4.7 members per family; monthly income approx. USD 239.00; food and transportation expenses approx. USD 153.00; small size 1 or 2-storey unfinished houses with 2 bedrooms and 0.8 bathrooms; no garden, garage or swimming pool; building occupies entire terrain without free areas between neighbors; paved or unpaved streets.
- Class E: 4.6 members per family; monthly income approx. USD 163.00; food and transportation expenses approx. USD 148.00; small size 1-storey unfinished houses with 1.7 bedrooms and 0.3 bathrooms built with low quality material; no garden, garage or pool; unpaved streets (bare soil).

The spatial distribution of label data was not uniform. Sample points were selected in homogeneous social class areas, independent of the land use. However, even during the field work, homogeneity was sometimes difficult to obtain because of the variety of constructions, building materials, surfaces, etc. The information collected is representative for an approximate radius of 50 m around a sampled point (GPS precision is around 15 m). The following characteristics were observed for each sampled point:

- Location: UTM and geographical coordinates.
- Social class: A, B, C, D and E (A is the richest and E the poorest class).
- Green areas: observed for residential areas as
  - ○ Houses with large green areas
  - ○ Houses with small green areas, or
  - ○ Houses with no green areas
- Surface type: different ground surface types, such as asphalt, cement, grass, bricks, tiles or bare soils.
- Building type: building types and sizes observed, e.g. 3–5 floor buildings and 2-floor houses with top floor unfinished.
- Land use:
  - ○ Residential areas
  - ○ Commercial areas (shopping centers, supermarkets, small grocery shops, repair shops, informal markets, etc.)
  - ○ Other areas (industrial areas, recreational areas, health, education and government buildings, etc.)

All in all, 500 points were taken within the study area. The number of survey points for each social class was 100.

3. Methodology

We used a GIS-based method to model socioeconomic classes that can easily add new urban components to the modelling. The methodological framework is as follows. First a land cover classification of the QuickBird image is performed. The resulting classified image is then analysed with GIS procedures for estimating poor to rich regions in the image according to socioeconomic class rules defined for the urban context in study. This approach follows the assumption that features representing socioeconomic classes in a city share common physical characteristics identifiable in a satellite image.

The study employed three applications: Erdas, ArcMap, and MatLab. The first is a geospatial imaging processing software package and the second is a widely used GIS package. The third is a system for matrix-based computation that can work with attribute tables. The use of Matlab in the GIS modelling process improves the efficiency and repeatability of the data processing pipeline.

3.1. Image classification

Conventional supervised classification techniques were applied in order to identify land cover features from the QuickBird satellite image of the study area. Supervised classification requires the choice of appropriate physical characteristics of socioeconomic classes to later estimate the social patterns in the city using GIS. The question to be addressed by our classification was which features should be chosen to obtain good estimations of the spatial distribution of homogeneous zones of socioeconomic classes within a city?

Taking into account physical characteristics of Lima, we chose to classify here the following land cover features: green areas, water bodies, paved streets, bare soils, high-quality buildings and low-quality buildings. Low-quality buildings can be differentiated from high-quality buildings by their different roof types (see characteristics of buildings in Sections 2.1 and 2.2.2). To classify the image into those six classes, the traditional minimum distance and maximum likelihood techniques were applied (e.g. Gibson and Power, 2000; Campbell, 2002).

The minimum distance algorithm allocates a pixel by its minimum Euclidean distance to the centroid of each class. The pixel is assigned to the closest class, or marked as unknown if it is farther than a pre-defined distance from any class mean. Though if a pixel lies on the edge of a class, it might be that the value of the pixel is closer to the mean of a neighbour class and it will be assigned to the neighbour class.

The maximum likelihood classifier considers that the geometrical shape of the set of pixels belonging to a class can be described by an ellipsoid. Pixels are grouped according to their position in the influence zone of a class ellipsoid. The probability that a pixel will be a member of each class is evaluated. The pixel is assigned to the class with the highest probability value or left as unknown if the probability value lies below a pre-defined threshold.

It is important to define suitable training data for the categories considered within the urban area because of the variation in the spectral response of their components. For example, in the selection of a residential training sample all land cover types within a residential area have to be considered together as a residential class. Maximum likelihood is more sensitive to the quality of training data than the minimum distance technique. Training data that are not carefully selected may introduce error (Campbell, 2002).

3.2. Grid-based approach

The content of the resulting classified image is here examined with various GIS procedures in a grid-based approach. First, we vectorized the raster classified image, creating polygons for all land cover classes. The second step was to create an empty rectangular grid with unique cell IDs and grid cell size defined according to the required mapping and computational capabilities. We performed many tests for 50, 100, 200, 500 m, etc. cell sizes, using ArcMap v.9 and a Pentium desktop computer. We chose to create a grid with cell size of 1 km $\times$ 1 km, because the computations with smaller cell sizes went out of memory. The cell matrix contained 11 rows and 9 columns (99 cells in total). The dataset was still quite large, having tens of thousands of data records for each cell. The third step was to intersect the vectorized classified image with the empty grid to serve as a base map. The combination of urban features within each grid cell was then analysed to determine the socioeconomic class of each cell. The fourth step was to compute for each cell the percentage of land cover types within it and to store the results in a new attribute table. Various other urban

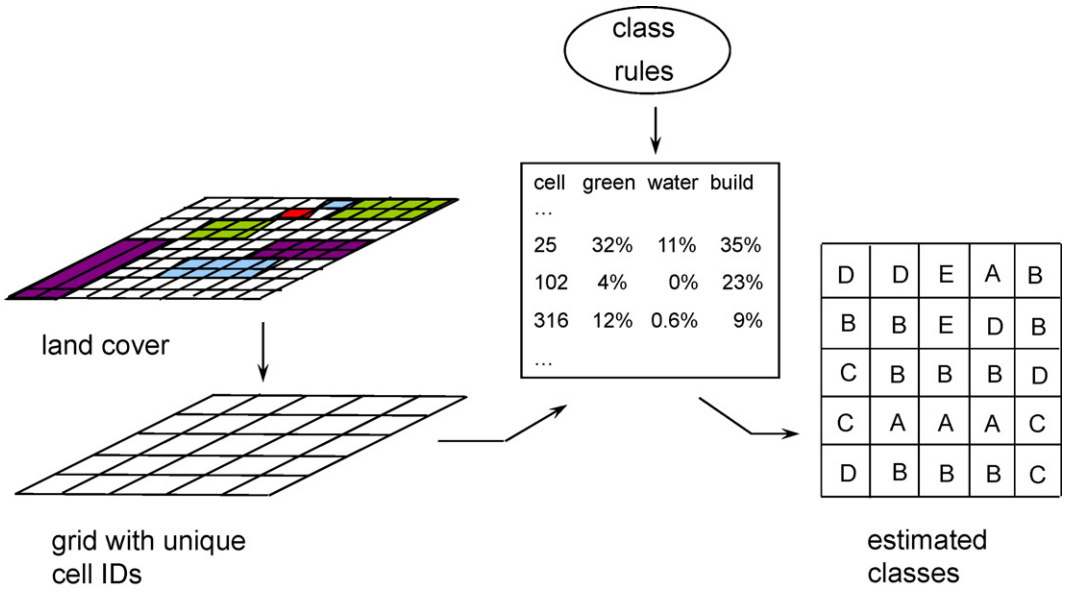

Fig. 3. Grid-based approach for categorizing grid cells according to their content.

features within the cell can be considered as appropriate in this step. The final step was to analyse the combination of measurements of urban features within each cell to obtain an estimation of socioeconomic classes. Steps 4 and 5 were done with help of MatLab. Then we performed a spatial join of the intersected grid-shaped polygon layer containing land cover data and unique cell IDs with the new table containing socioeconomic classes thus creating a layer that contained both unique cells IDs and socioeconomic classes.

Fig. 3 shows a diagram with an overview of the grid-based modelling approach. The grid-based approach enables one to analyse, add and subtract land cover types and other urban components of socioeconomic classes in order to find local class rules.

In this study, we applied to each cell of the base map membership rules to obtain a differentiation of spatial patterns of socioeconomic classes. Considering the study area description and the physical characteristics of social classes in Lima, the following rules were derived:

- Class A: presence of many green areas and many water bodies.
- Class B: presence of some green areas and a few water bodies.
- Class C: some green areas, no water bodies and more high-quality buildings than low-quality ones.
- Class D: a few green areas, no water bodies and more low-quality buildings than high-quality ones.
- Class E: very few green areas, no water bodies and more low-quality buildings than high-quality ones.

3.3. Accuracy assessment

An accuracy assessment was performed on the estimation results of socioeconomic classes by comparing them with the reference data from the ground truth. Accuracy assessment is itself a difficult issue, especially of large area maps, as is the case here (Foody, 2002). A confusion or error matrix was chosen because it is the most widely used method of statistical measure of accuracy in the remote sensing literature. It provides a quantitative metric of accuracy depicting the classified categories versus the field-observed values.

The agreement/disagreement between the estimation map and the reference data is given by an overall accuracy value and by a kappa coefficient, which is useful to determine the disparity between the estimated data and the reference data (Lavigne et al., 2006). Two types of thematic errors can be measured in a confusion matrix. They take into account the accuracy of individual categories. One is given by the producer's accuracy, which indicates the proportion of ground base reference samples correctly assigned. It details errors of omission, i.e., when a pixel is omitted from its correct category. The other error is given by the user's accuracy, which indicates the proportion of data from the estimation map representing that category on the ground. It is a measure of errors of commission, i.e., when a pixel is committed to an incorrect category.

We call attention to the fact that the ground truth data upon which the confusion matrix is to be based is of major importance, because it has serious implications to the accuracy assessment. The sampling design to acquire sampled points should cover adequately the area and generate sufficient samples for each of the map classes. Therefore, in addition to providing the confusion matrix, it is also important to consider the reliability of the sampling design and the confidence in the ground data labels (Foody, 2002).

4. Results

4.1. Land cover classification

Figs. 4 and 5 show an enlargement of an area in the image with rich and poor classes and the resulting classified images with the minimum distance and maximum likelihood algorithms. Both classification methods display errors, but as approximative solutions they yielded good results.

The maximum likelihood technique determined more water bodies than the minimum distance approach, but fewer green areas, which were mostly taken as high-quality buildings in the maximum likelihood (see Fig. 5). The minimum distance method came up against its limits within the high structured urban housing zones in the central sector of the image, where residential houses, commercial buildings, sidewalks, streets, bare soils and other urban features occur. But it recognized well streets and bare

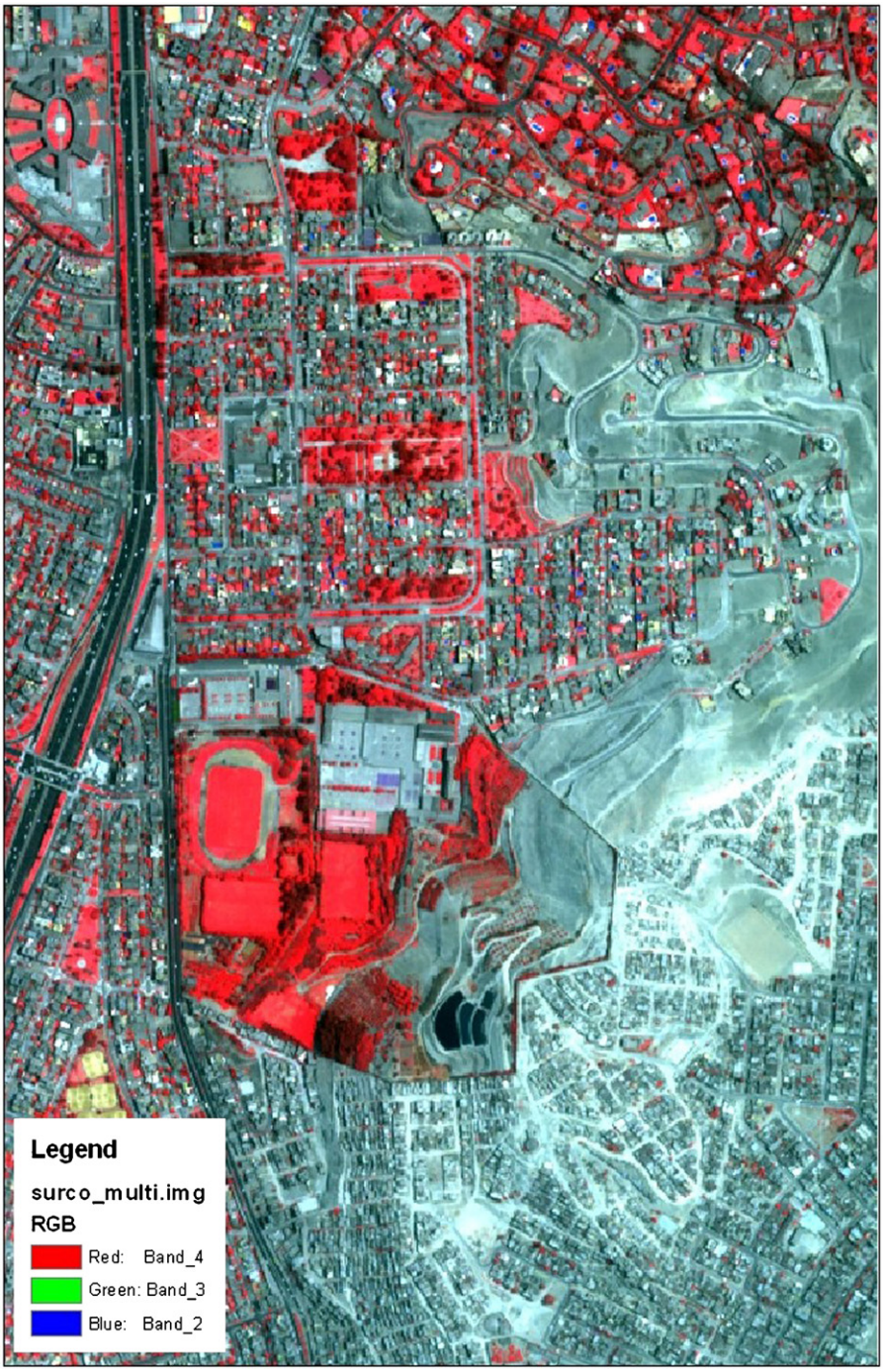

Fig. 4. Zoom of an area of the satellite image with rich and poor classes.

soils. The different shapes and colours present in slums (low-quality buildings) determine a complex urban formation, which is difficult to differentiate from other land cover types, especially bare soils and streets, which may present similarities in surface and roof material. The minimum distance technique presented more difficulties to distinguish low-quality buildings from streets (Fig. 5a). In the maximum likelihood result (Fig. 5b) low-quality buildings zones were almost completely found in the southeastern sector of the image, where slums are indeed present, but also in other regions of the image, due to their confusion with streets and other urban features, exposure to bare soils, and computational errors.

4.2. Estimation of social classes

The two images in Figs. 6 and 7 show the resulting estimated geographic pattern of socioeconomic classes in the study area. The estimation is based on the land cover classification previously shown in Fig. 5a and b, respectively. The ground truth data was also included in the images.

Compared visually to the ground truth, both results present a reasonable estimation of socioeconomic classes. Both images display a large area with social class A – lots of green and water – at the upper part of the study area. Poor settlements – classes D and E, with almost no green and no water – were found mainly in the

southeastern part of the study area, which correspond to the reality in Lima. Slums are mostly clustered on the inferior part of the hill on the right side. Out of poor areas, class B samples are quite widely spread out in the image, just as are class B cells in the resulting images. Note that social class C ground data and estimated cells appear mainly on the borders of poor settlements.

The social classes of the reference data have in many places a smaller spatial pattern than the 1 km grid. For example, the sample points in the southeastern region change between classes C, D and E within a few 100 m. This high spatial heterogeneity cannot be precisely projected by homogeneous 1 km-grid cells, which were mainly considered classes E and D.

In the following section we report the statistical comparison with the ground truth.

4.3. Confusion matrix

The accuracy assessments of the maps in Figs. 6 and 7 are given in the confusion matrix presented in Tables 1 and 2, respectively. The confusion matrix is used here mainly to provide more information about the approach applied and to make a comparison possible between the two resulting maps. The constant number of points sampled for each class, i.e., 100 points, allows one to make a straightforward comparison of the results. However, since these

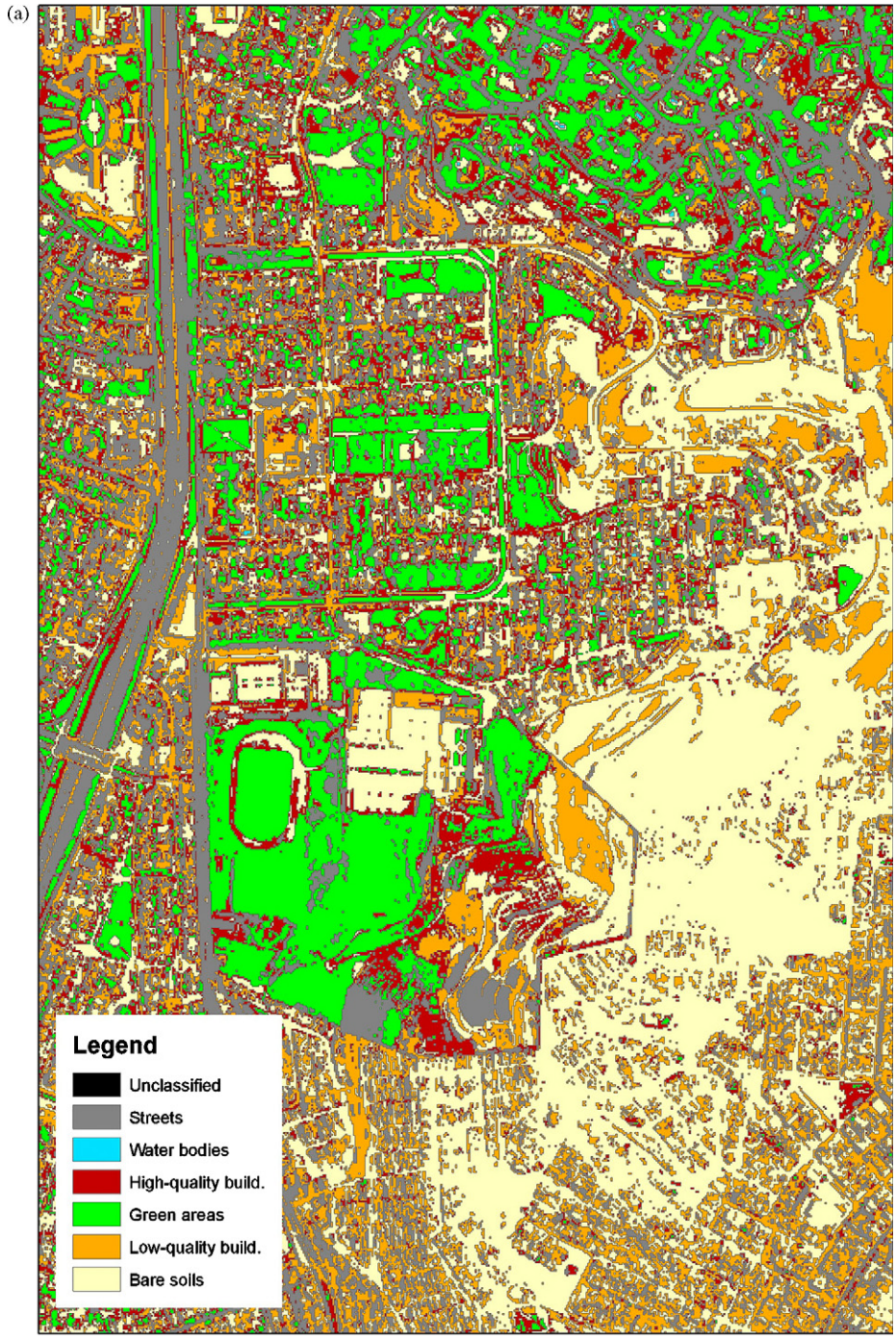

Fig. 5. Resulting images of classification with (a) minimum distance technique, and (b) maximum likelihood technique.

(b)

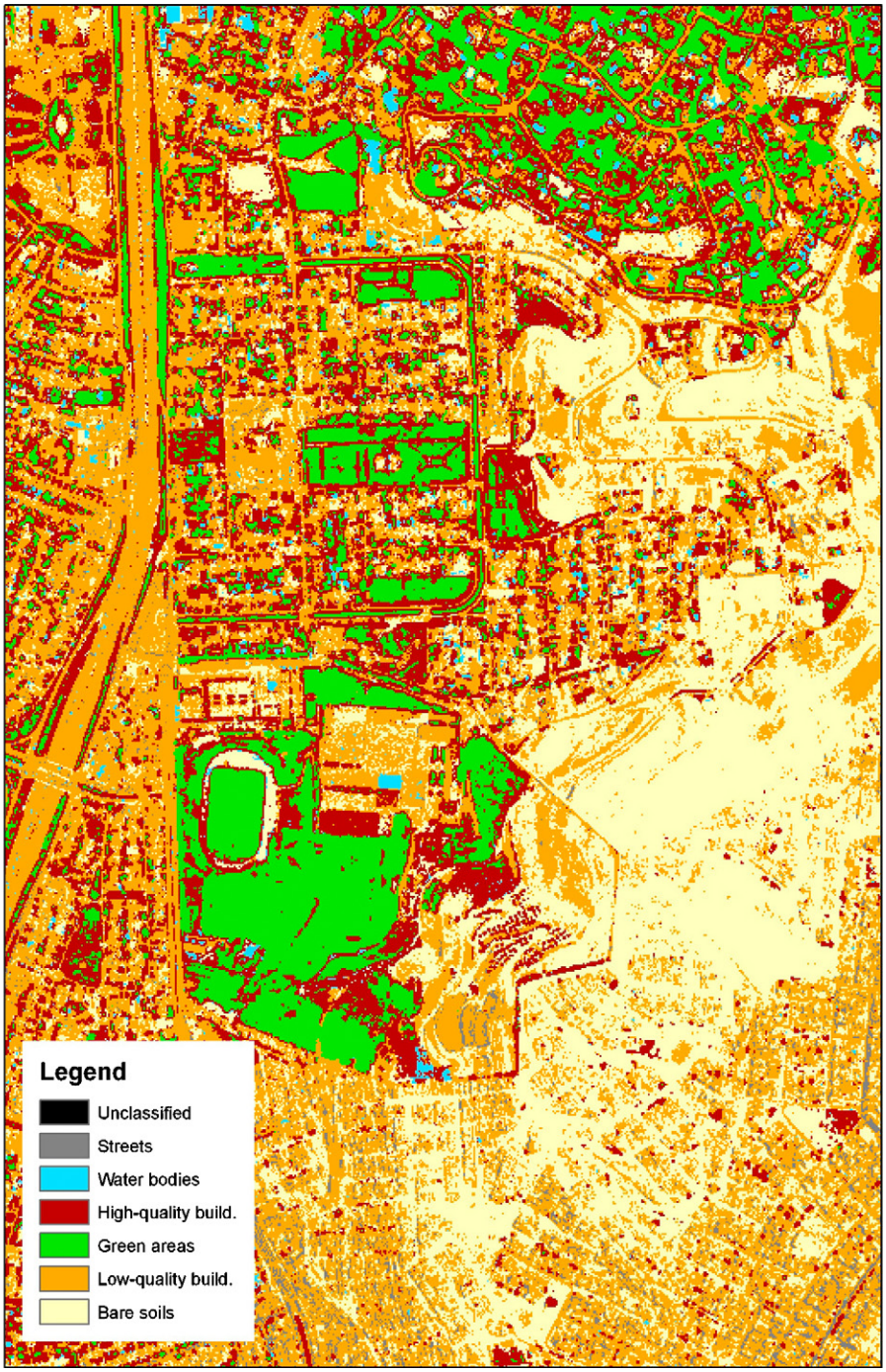

Fig. 5. (*Continued*).

points were sampled by different people and the differentiation between socioeconomic classes is not always obvious, especially in spatial transition areas between classes B and C, C and D, and D and E, some points had practically the same location and were labelled with similar but different socioeconomic classes.

The overall accuracy shows an average of only 40% of actual classes recognized, due to misclassification and to the sampling points for computing accuracy assessment. However, it does not mean that individual classes were correctly classified only at this rate. The kappa value is high, so the disparity between the estimated data and the reference data is small—agreement is easy to achieve. The higher the kappa, the 'less random' is the classification.

Tables 1 and 2 indicate that A classes had the highest accuracy. Class A green areas and water bodies were identified quite well by both supervised classification methods. In contrast, low-quality buildings in class E displayed the lowest accuracy values. The estimated cells indicate that a few vegetation and water bodies were found in areas of class E, which were regarded as class D or C. Notice how there was a lot of confusion between social classes D

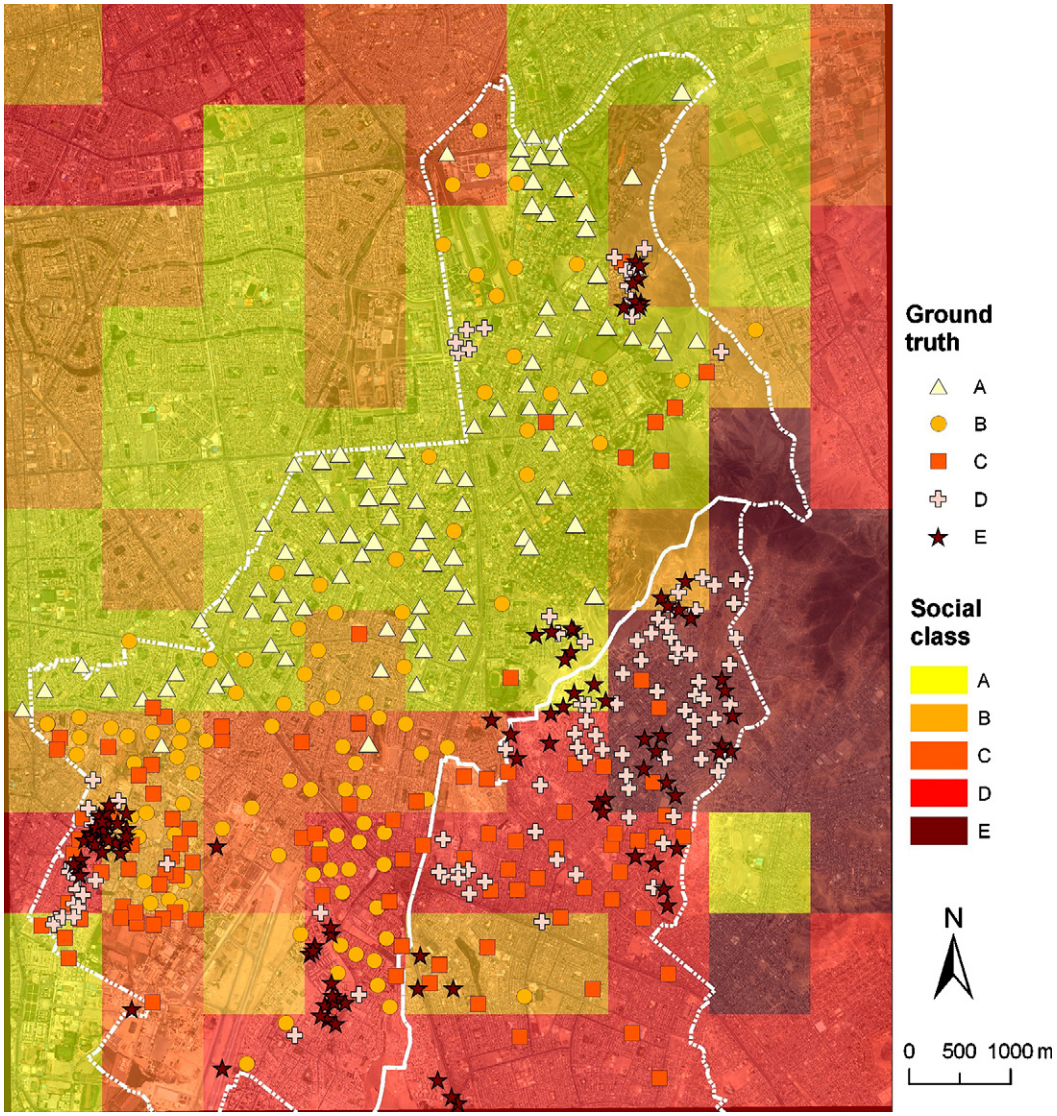

Fig. 6. Square grid with estimated socioeconomic classes for the image classified with minimum distance.

and E. Most errors in the matrix are actually between relatively similar classes, i.e., A and B, B and C, C and D, and D and E.

Many human activities such as commercial buildings and industrial land are present in classes C and B, which yielded a moderate accuracy value. The percentage of land covered by classes B and C may vary significantly with the amounts of vegetation and water considered for these classes. In the map of Fig. 6 class C had more difficulty in being identified than in Fig. 7, being mostly considered class D. This suggests that less water bodies and vegetation were found in map 6, which is in accordance with the minimum distance classification.

The accuracies for classifying socioeconomic levels B, C, D and E in the map of Fig. 7 are higher than in the map of Fig. 6. For example, class C has a producer's accuracy of 50%, meaning that 50% of the reference data were found to be classified as class C. On the other hand, the user's accuracy is only 38.76%, meaning that only 38.76% of the map data classified as class C can be expected to be class C when visited on the ground. When the user's accuracy is higher than the producer's accuracy, e.g. in classes C and E of Table 1, it indicates an under-estimation of the proportion of covered area.

5. Summary

We have approached the problem of automatically identifying regions with different socioeconomic classes in urban areas of large cities by applying conventional supervised classification and GIS analysis techniques. We chose not to use specially tailored algorithms for classifying urban areas, because they are usually bound to a specific context and are not easily available. Instead, we aimed to develop a methodology that can be practically applied in governmental institutions and NGOs, particularly in developing countries, and not only in the academic environment. We estimated socioeconomic classes by considering a grid-based analysis of urban physical components of the land surface, which could be more easily adaptable to various contexts.

The traditional classification methods reach their limitations in urban systems due to the high spectral heterogeneity of urban features. The misclassification of some urban formations came therefore as no surprise, since high-quality buildings, slums, streets and their surroundings are very heterogeneous. We applied the GIS procedures to match the classified image with various grid cell sizes, but due to computational capabilities we chose to work

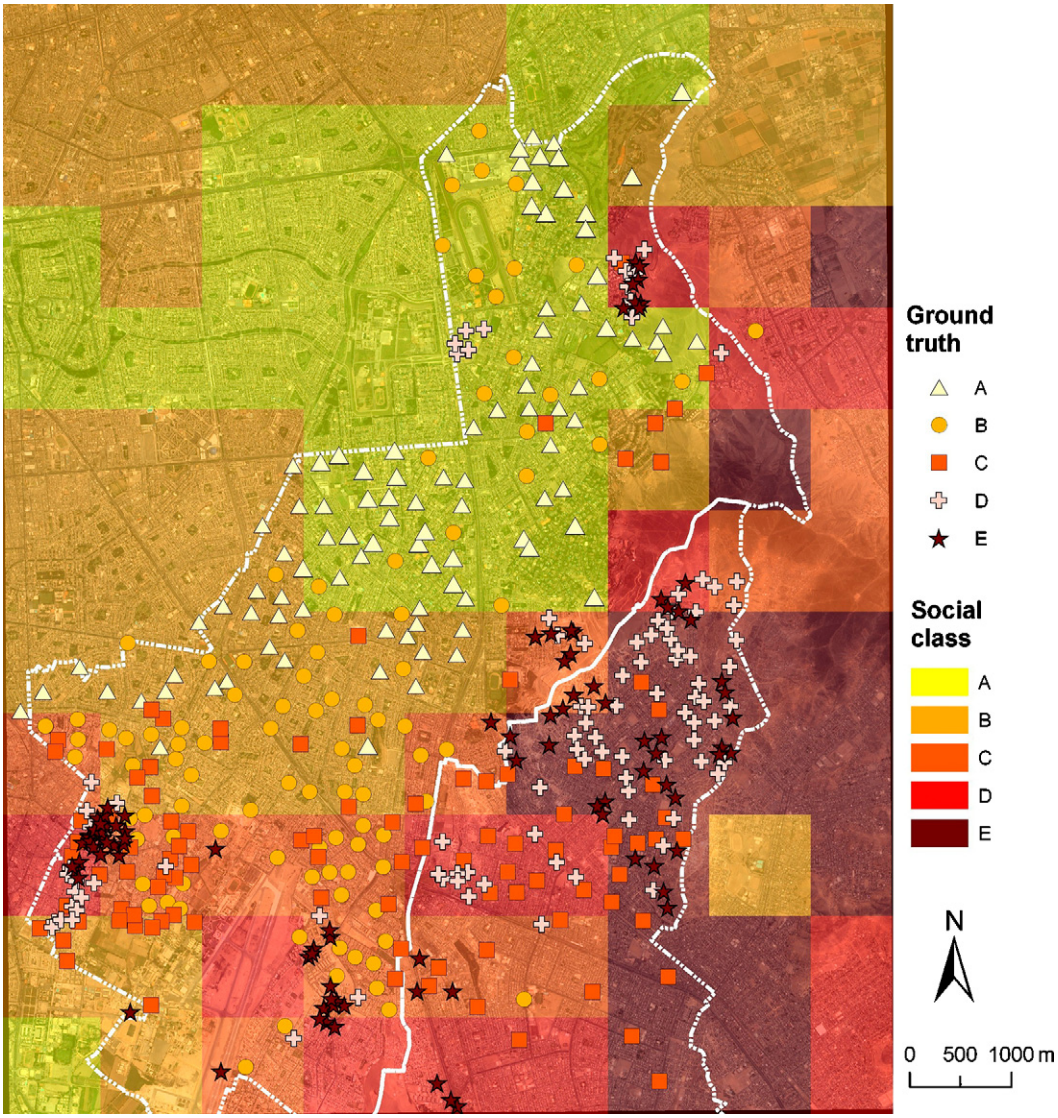

Fig. 7. Square grid with estimated socioeconomic classes for the image classified with maximum likelihood.

with 1 km-cells, which can find good approximate solutions and support many urban planning decisions. The 1 km × 1 km cells generalization is good – not too small, not too large – especially for producing estimative maps for a whole city.

The joint use of ArcGIS and MatLab brought efficiency and flexibility into the modelling process, which became faster and more reproducible. To build an automated data process pipeline, a great deal of custom programming would be needed.

Table 1
Confusion matrix of the resulting estimated classes for the grid-based approach with minimum distance classifier

Ground truth	A	B	C	D	E	Total
Classified as						
A	94	26	11	13	10	154
B	4	36	28	14	25	107
C	2	18	16	0	3	39
D	0	20	42	39	46	147
E	0	0	3	34	16	53
Total	100	100	100	100	100	500
Producer's accuracy (%)	94	36	16	39	16	
User's accuracy (%)	61.04	33.64	41.02	26.53	30.19	
Overall classification accuracy (%)	40.2					
Kappa value	0.91					

Table 2
Confusion matrix of the resulting estimated classes for the grid-based approach with maximum likelihood classifier

Ground truth	A	B	C	D	E	Total
Classified as						
A	67	21	1	6	0	95
B	33	41	19	1	1	95
C	0	36	50	11	32	129
D	0	2	24	41	40	107
E	0	0	6	41	27	74
Total	100	100	100	100	100	500
Producer's accuracy (%)	67	41	50	41	27	
User's accuracy (%)	70.53	43.16	38.76	38.32	36.49	
Overall classification accuracy (%)	45.2					
Kappa value	0.9					

The accuracies of the estimated socioeconomic classes were summarized in the confusion matrices in Tables 1 and 2. The socioeconomic estimation encountered some problems when the grid cell values were compared to the sampled data. The matrices revealed interclass confusions, which could be resolved with the use of additional discriminatory information on the socioeconomic classes and the use of smaller grid cells. The accuracy assessment sites of homogeneous social classes should be an accurate representation of the ground conditions, but this is rarely the case. Some practical constraints should be therefore considered in order to not reduce the credibility of the accuracy statement derived. For example, a single, precise definition of the characteristics of social classes should be known by all involved in the sampling of data, as well as a definition of how to categorize bare soils, public places and other urban features, which could take the class of regions around them.

6. Conclusions

The methodology described allows the rapid assessment of socioeconomic classes in large cities and can be performed on any desktop computer with common remote sensing and GIS software installed. The study focused on the characteristics of Lima/PE; however, the modelling framework can be applied to any other similar urban area, particularly in large cities of Latin America, where ground truth data is often not available and contrasting socioeconomic classes co-exist and are identifiable through physical characteristics in land cover data of the urban system.

The main urban components of socioeconomic classes in this paper have been green areas, water bodies, bare soils, paved streets, high-quality buildings and low-quality buildings. These components could still be refined further, for example, with green areas taking into account water use levels and energy consumption for each social class. A number of other urban components that are also likely to affect environmental quality could be also used, e.g. traffic congestion, waste disposal and population density. New urban features can easily be added to the proposed framework and combined into a grid cell, in order to indicate the environmental impacts as required.

The methodology described could be applied with other very high resolution sensor data of urban areas, which have been widely available at reasonable costs and with frequent updates, e.g. Google Earth.

We assume that smaller grid cells, ideally 50 m $\times$ 50 m, would increase the quality of the applied method, because the natural spatial pattern of social classes in Lima is very heterogeneous, leading to classification errors on a 1-km-scale. We expect that upgraded hardware and software will allow perform efficiently the necessary calculations for smaller cells. Therefore, further work will focus on getting a higher degree of geometric accuracy in the estimation of socioeconomic classes.

We plan also to compare the results presented here with other results obtained by using different classification algorithms, such as neural network (Tapiador and Casanova, 2003) and support vector machine (Landis et al., 2005; Huang et al., 2002).

References

APOYO, 2005a. Perfiles zonales de Lima Metropolitana. APOYO Opinión y Mercado, Lima, 114 pp. (in Spanish).

APOYO, 2005b. MAPINSE de Lima Metropolitana 2005 – IV, Distritos de Santiago de Surco y San Juan de Miraflores. APOYO Opinión y Mercado, Lima, 9 pp. (in Spanish).

Barros, J., 2004. Urban Growth in Latin American Cities: Exploring Urban Dynamics through Agent-based Simulation. PhD Thesis. University College London, 289 pp.

Campbell, J.B., 2002. Introduction to Remote Sensing, third ed. Taylor and Francis, London.

Foody, G.M., 2002. Status of land cover classification accuracy assessment. Remote Sensing of Environment 80, 185–201.

Fox, J., Rindfuss, R.R., Walsh, S.J., Mishra, V. (Eds.), 2003. People and the Environment: Approaches for Linking Household and Community Surveys to Remote Sensing and GIS. Kluver Academic Publishers, Massaschusetts, US.

Gibson, P.J., Power, C.H., 2000. Introductory Remote Sensing: Principles and Concepts + Digital Image Processing and Applications. Taylor and Francis Group, Routeledge.

Herold, M., Hemphill, J., Clarke, K.C., 2007. Remote sensing and urban growth theory. In: Wang, Q., Quattochi, D.A. (Eds.), Urban Remote Sensing. CRC Press, Taylor and Francis Group, Boca Raton, US.

Huang, C., Davis, L.S., Townshend, J.R.G., 2002. An assessment of support vector machines for land cover classification. International Journal of Remote Sensing 23 (4), 725–749.

Jensen, J.R., Cowen, D.C., 1999. Remote sensing of urban/suburban infrastructure and socio-economic attributes. Photogrammetric Engineering & Remote Sensing 65 (5), 611–622.

Landis, F., Avelar, S., Orbanz, P., Zah, R., Buhmann, J., 2005. Preparatory study for the Seed Project. Internal Report, Swiss Federal Institute for Materials Testing and Research (Empa), Switzerland.

Lavigne, D.A., Hong, G., Zhang, Y., 2006. Performance assessment of automated feature extraction tools on high resolution imagery. In: MAPPS/ASPRS 2006 Fall Conference, Nov. 6–10, San Antonio, Texas.

Lyndolph, P.E., 1973. On the causes of aridity along selected group of coasts. In: Aminan, D.H.K., Wilson, A.W. (Eds.), Coastal Deserts—Their Natural and Human Environments. The University of Arizona Press, pp. 62–72.

Mesev, V., 2003. Remotely Sensed Cities. Taylor & Francis, London.

Shutz, E., 1996. Ciudades en América Latina: desarrollo barrial y vivienda. Santiago de Chile, Ediciones Sur. (in Spanish).

Sembler, C.R., 2006. *Estratificación social y clases sociales. Una revisión analítica de los sectores medios*. ONU, CEPAL, División de Desarrollo Social, Serie Políticas Sociales 125, 75 pp. (in Spanish). http://www.eclac.cl/publicaciones/xml/6/27586/sps125_lcl2637.pdf.

Stefanov, W.L., Ramsey, M.S., Christensen, P.R., 2001. Monitoring urban land cover changes: an expert system approach to land cover classification of semiarid to arid urban centers. Remote Sensing of Environment 77, 173–185.

Sutton, P.C., Taylor, M.J., Anderson, S., Elvidge, C.D., 2007. Sociodemographic characterization of urban areas using nighttime imagery, Google Earth, Landsat, and "social" ground truthing. Urban Remote Sensing, CRC Press, pp. 291–310.

Tapiador, F.J., Casanova, J.L., 2003. Land-use mapping methodology using remote sensing for the regional planning directives in Segovia, Spain. *Landscape and urban planning* 62 (2), pp. 103–115, Elsevier Science, Amsterdam.

Taubenbock, H., Esch, T., Roth, A., 2006. An Urban Classication Approach on an Object-Oriented Analysis of High Resolution Satellite Imagery for a Spatial Structuring within Urban Areas. Workshop of SIG Urban Remote Sensing. Humboldt-University, Berlin, 2–3 March, 2006.

UN, 2006. World Urbanization Prospects: The 2005 Revision. United Nations, New York, 185 pp. http://www.un.org/esa/population/.

Wang, Q., Quattrochi, D.A., 2007. Urban Remote Sensing. CRC Press, Taylor and Francis Group, Boca Raton, US.

Zhang, G., Foody, G.M., 2001. Fullly-fuzzy supervised classification of sub-urban land cover from remotely sensed imagery: statistical and artificial neural network approaches. International Journal of Remote Sensing 22, 615–628.